

Original Research Article

Geospatial Assessment of Landslide Risk Susceptibility Using Frequency Ratio and Remote Sensing in the Tropical River Basin of the Western Ghats

ABSTRACT

Wayanad is prone to unexpected landslides due to human interventions s and, unusual geological and abundant rainfall, which cause loss of life and property damage. This study was conducted to construct a landslide susceptibility map of the Kabani River Basin area in the Southern Western Ghats region using a statistical method. For this, we used previously recorded landslide locations, and 11eleven landslide factors were used for modelling, namely lithology, geomorphology, slope angle, soil texture, distance from streams, distance from roads, distance from landmarks, topographic wetness index (TWI), rainfall, land use/land cover, and slope curvature, which were extracted from the spatial database.

Initially, the study presented eds a very comprehensive approach by mapping landslide-prone areas using relative frequency and prediction rate, which generated s a Landslide Prone Area Index (LSI) and a susceptibility map. Furthermore, the study revealed eds that the southwest part of the study area is prone to landslides because due of to the extensive influence of the 65° slope, intense rainfall, soil texture, topography moisture index, curvature, lithology, and geomorphology. It also includes the distances s to roads, lines, s and streams. The predicted pattern is highly similar to the area where landslides have occurred in the past, and it helps in future conservation planning and sustainable land use planning to mitigate landslide risk in the south-western Western Ghats.

Keywords: Landslide Susceptibility, Frequency Ratio (FR), Remote Sensing (RS), Western Ghats, Land Use/Land Cover (LULC)

Commented [SA1]: LSI stands for "Landslide Susceptibility Index".

Commented [SA2]: Consistency: Different forms of this word have been used in the text.
'southwest' no space [2 times]
'south-west' with hyphen [1 time]
Please pick one style and use it consistently throughout the text.

1. INTRODUCTION

A common but devastating natural disaster, a landslide, represents the downward and outward movement of slope-forming materials, such as rock, soil, and debris. (Gerrard 1994). Landslides occur when the stability of slopes is compromised by natural and anthropogenic factors. The sheer force of a landslide can have devastating consequences, including loss of life, damage to infrastructure, and significant economic losses. (A. Saha et al. 2023; Tien Bui et al. 2012; Nadim et al. 2006). The underlying causes of landslides are multifaceted, including seismic conditions, hydrological changes, seismic activity, and human interventions, leading to natural imbalances. Mountainous areas around the world are prone to landslides, and as a measure, from 1995 to 2014, more than 3850 landslides were recorded, resulting in the loss of more than 11,500 human lives and the death of approximately 1,63,500 people. (Haque et al. 2019). It has been recorded that approximately 95% of landslide incidents occur in developed countries and cause damage of 0.05% of the country's annual income. (Glade et al. 2005). Therefore, it is necessary to take decisive and effective steps to adopt precautionary measures and mitigation measures related to landslides. Landslide hazard assessment and mapping are crucial processes for understanding and mitigating landslide-related risks. Sensitivity assessment regarding the spatial division of landslide-prone areas depends on the topographic-ecological situation. (Merghadi et al. 2020).

Growing awareness of landslide impacts and the need for urban development in challenging mountainous terrain has increased scientific interest in LSZ mapping. (Batar and Watanabe 2021; Chawla et al. 2019; Dikshit et al. 2020; Peethambaran et al. 2020; Pham et al. 2017). LSZ mapping methods have evolved by incorporating heuristic, semi-quantitative, statistical, or probabilistic approaches. (Shano et al. 2020). In the coming era, and still today, machine learning (ML) algorithms have gained importance as advanced tools for modelling complex relationships between geo-ecological components (Pham et al. 2016a, b; Pradhan, 2013a). Despite their many advantages, these algorithms often do not perform well and currently face several limitations, such as the low interpretability of the influence of factors, the possibility of overfitting in unbalanced datasets, and high computational requirements. (Hong et al. 2019; Pradhan et al. 2023; Tang et al. 2023). These challenges underscore the critical need for expert validation to improve the reliability and practical applicability of these models. Conversely, while explainable, methods based solely on expert opinions may introduce biases and variations. (Erener et al. 2016; Yalcin 2008).

The objective of this research is to explore the effectiveness of using the frequency ratio model and prediction rate to analyse the landslide hazard of the Kamati River, a tributary of the Cauvery River that flows through southern India. The main objective of this research is to identify their strengths and weaknesses and explore their potential to influence successful risk reduction measures. In this studywork, a comprehensive point mapping of landslide susceptibility in this area using the relative frequency (RF) and prediction rate (PR) is reported.

The site is a hilly area that has already experienced several landslides, mainly in the south-western part, and no research has been conducted in this area of the basin or the region situated in western the part of the basin that has ever been done. Therefore, determining the condition of slopes and identifying

Commented [SA3]: Kindly, expand the abbreviation once.

landslide-prone areas iswere a crucial tasks. This se study presents a very-comprehensive approach forby mapping landslide-prone areas using relative frequency and prediction rate, which generates a landslide-prone area index (LSI) and a susceptibility map. The evaluation of the model's effectiveness of the model and the identification of high-risk areas on the south-western slopes of the Kabani River Bbasin provide valuable insights into precautionary measures to mitigate the impact of landslides due to the nature of rainfall and erosion. By improving landslide anticipation and management, this research contributes to the reliability and safety of the region, not only in the studied region, a but also beyond its geographical boundaries.

2. MATERIALS AND METHODS

In this study, a landslide occurrence table was created by collecting as much data as possible on recent and past landslides, and evaluating the relationship between each conditioning factor and landslide probability. Using the provided methodology chart (Figure 1), the landslide probability was assessed, and the main factors that have-caused landslides in the past were identified. The frequency ratio model was used to predict the probability of their occurrence in the future, owing due to the influence of the same factors.

2.1 Methodology

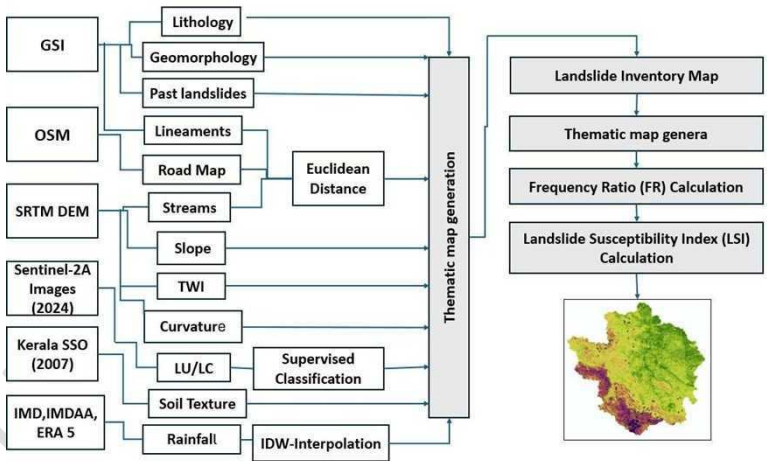


Fig 1: Methodology of Frequency ratio

2.2 Frequency ratio (FR) method

The FR method is used to rely on the concept of a favourable function and to calculate the statistics between previous landslides and the occurrence of landslides, and the statistics between the conditioning factors of the landslide (Chung and Fabbri 1999; Vijith and Madhu 2008). Values greater than FR 1 indicate a strong relationship between the factor and the occurrence of landslides, whereaswhile a value below 1 reflects a weak relationship (Lee and Sambath 2006; Vijith and Madhu 2008; Sharma and Mahajan 2018).

Commented [SA4]: Different styles have been used when citing figures in the text.
'Figure(s)' [1 time]
'figure(s)' [1 time]
'Fig(s).' [3 times]
Please pick one style and use it consistently throughout the text.

Commented [SA5]: FR (>1)

A contingency table was prepared to calculate the corresponding FR for each landslide conditioning factor, and the ratio of landslide occurrence to non-occurrence was calculated using Eqs. (1), as follows:

$$W_{ij} = FL_{ij} / FN_{ij} \quad (1)$$

where W_{ij} is the FR of the i th class attribute of the j th causal factor, FL_{ij} is the FR of the landslides that occurred in the i th class of the factor j , and FN_{ij} is the FR of the non-occurred landslides in the class ' i ' of the factor ' j '. The landslide susceptibility index (LSI) was computed by the summation of the FRs of all the landslide conditioning factors, followed by Eq. 2. $LSI = \sum W_{ij}$ (2)

3. STUDY AREA

The Kabani River is an eastward-flowing river (KRB area=1685 km²), an integral part of the southern Indian Cauvery River system, also known as Dakshina Ganga. The selected drains were in between the latitudes of 11°29'37.75"N and 11°59'5.93"N and the longitudes of 74°46'44.54"E and 76°18'1.26"E (figure 2). The KRB characterized the dendritic pattern, and the channel was in the 7th order. The Kabani River originates from the northern Wayanad high range of elevations (2140 m above MSL) from the Western Ghats, by the confluence of two rivers, the Panamaram and Mananthavady Rivers. Wayanad is a tableland in the state of Kerala, with the elevations ranging from 700 to 2100 meters above the Mean Sea Level, in the state of Kerala. The regional geology is dominated by Precambrian rocks, and the predominant rock types include gneisses, schists, and granites (Nagaraju and Papanna, 2009).

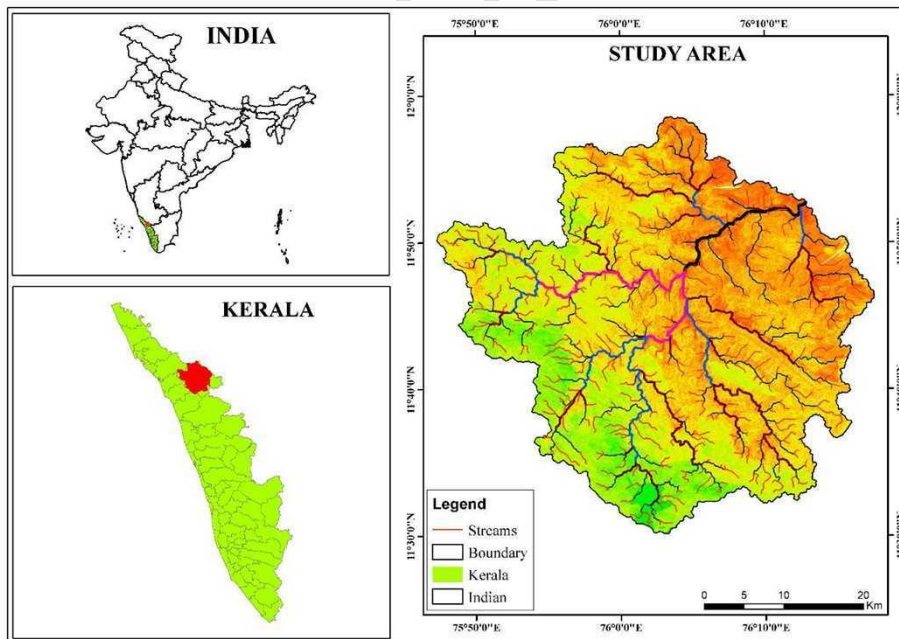


Fig 2. Location Map of the Study Area

The Wayanad Plateau is very complex, it leads to the formation of different landscapes through tectonic activities of tectonics such as faults, folds, and joints, and also continues denudation activities moulding their structure. The following climate of the KRB in the predominant tropical monsoon condition is, characterized by distinct wet and dry seasons, with marked high temperature variation.

The period from June to September results in a high amount of precipitation, while the post-monsoon period from October to November experiences a reduction in the quantity of rainfall. The mean annual rainfall is extended between the range of 1200 mm and 2500 mm. Rainfall is more in the south-west, as it moves to the north-east, it moves from a heavy to low rainfall distribution. The highest temperature is found along the gently undulating terrain of the plateau, and the mean annual temperature is between 22.5°C and 35.8°C (Achu et al., 2021). This remarkably controls the region's hydrological pattern, and it is also directly influenced by the diverse soil types, from clay to loam in texture. It together promotes the different land-use practices, such as agroforestry, paddy, plantation crops, and tree plantations.

The study area is rich in diverse systems and lush topography aligned with evergreen and deciduous forests in the Western Ghats, and this region (Anoop and Ganesh., 2023) supports a wide range of flora and fauna, including several types of endemic and endangered species.

4. RESULTS AND DISCUSSIONS

4.1 Data preparation and Landslide causative data and Factor selection

4.1.1 Lithology

Lithology is a major factor that directly controls landslide events, and variations in its composition also cause changes in the permeability of rocks and soil, which controls slope stability (Kavzoglu et al. 2014). The study area, which is associated with the Precambrian Metamorphic Shield of Southern India, reveals the dominance of high-grade metamorphic rocks.

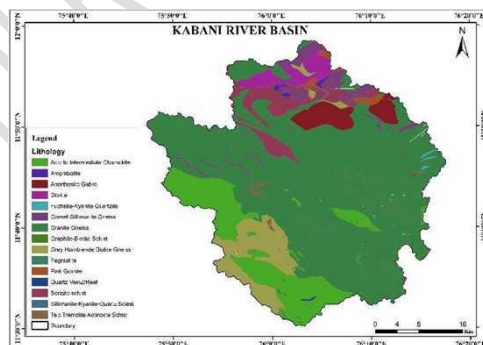


Fig: 3 Lithology

4.1.2 Geomorphology

Commented [SA6]: It is better to write as "Data Preparation and Landslide Causative Factors"

Commented [SA7]: Figure labels are not uniform. Kindly check for all figures.



Commented [SA8]: Geomorphology image is missing. Wrong image placed.

Commented [SA9]: Mentioned range in not matching the legends of the image. Also it recommended to categorise the legends as mentioned.

The porosity and permeability of soil play a crucial role in the case of shallow landslide acceleration. In this region, the majority of the previously occurred landslides through were the influence by of intense rainfall triggered by the excess pore-water pressure generated in the soil (Kuriakose et al. 2009). Four soil textural classes characterize the soils of the study area, viz., clay (69.43% area), loam (18.36%), gravelly clay (11.28%), and gravelly loam (0.93%) (Fig. 4c).

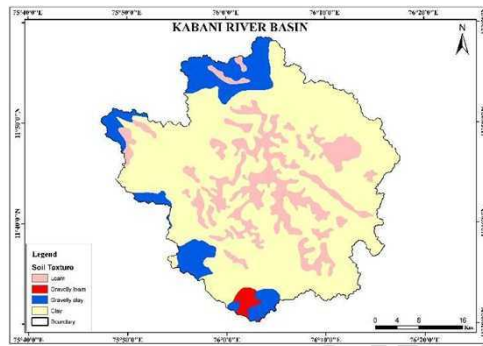


Figure 4c, Soil Texture, source: Kerala State Survey Organisation

4.1.5 Slope Curvature

The curvature of the slope signifies the morphology, convergence, and divergence of the surficial water flow and identifies the slope stability (Ding et al. 2017). The normal curvature is a combination of the plan curvature and profile curvatures, which was established in this study. Convex slopes are often considered more stable than compared to concave slopes because the former quickly drains the water into the lower slope area, whereas while the latter is more likely to be unstable because water concentrates on the lower slope, leading to slope instability. (Stocking 1972).

Commented [SA10]: Please check whether it is slope curvature, plan curvature, profile curvature, or curvature only. Also make sure the legends of the image matches the texts mentioned.

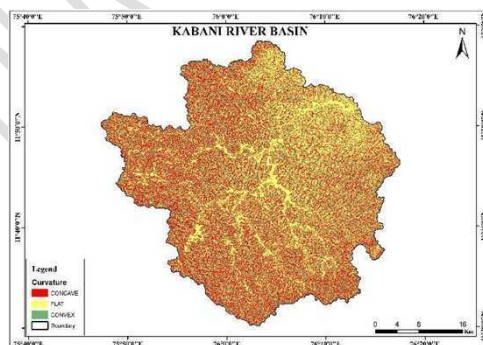


Figure. 4d, Curvature, source: SRTM DEM

4.1.6 Topographic Wetness Index (TWI)

One of the important topographic variables is TWI, which indicates the saturation and runoff concentration of the soil (Beven and Kirkby 1979). The TWI was calculated based on the local slope and upslope contributing area affecting the soil moisture content in a calculation unit, where α represents the upslope area and β represents the slope angle (Devkota et al. 2013). The TWI of the study area was reclassified into three classes. We classified the values as low, medium, and high for the analysis purposes, that is, < 5 , $5-10$, and > 10 , respectively.

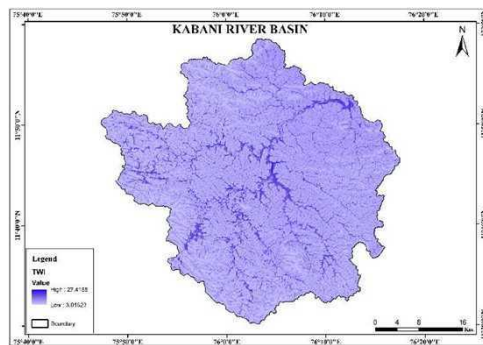


Figure. 4e: Topographic Wetness Index, source: SRTM DEM

4.1.7 Land use/Land cover

Specifically, in rugged landscapes, unplanned land use/land cover modification often leads to topographic changes that affecting slope stability (Kayastha et al. 2013). The land use/land cover map was generated using the Sentinel 2A satellite images. Among the different land use/land cover types, Coffee agro-forestry (40.82%) was dominant, followed by Deciduous Forest (20.88%), Agriculture (12.00%), Evergreen Forest (11.84%), Tea (4.96%), Barren land (4.29%), HA Grasslands (1.27%), Paddy fields (1.09%), Water bodies (1.03%), Tree plantations (1.00%), Built-up areas (0.55%), and Forest plantations (0.26%).

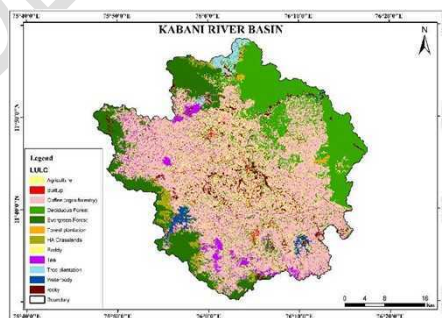


Figure.4f: LULC, source: Sentinel 2A Image

4.1.8 Rainfall

This nature of rainfall events is the most critical landslide triggering factor in the southern WG, and along with the majority of past landslide occurrences in the region were correlated with extreme rainfall events (Thampi et al. 1995). The rainfall choropleth map was generated using the IDW technique, and through the rainfall data of twenty-four rain gauge stations for 2019 were collected from the IMD. The annual rainfall over the area was reclassified into three zones; namely, < 2500 mm, 2501–3500 mm, and > 3501 mm for the analysis.

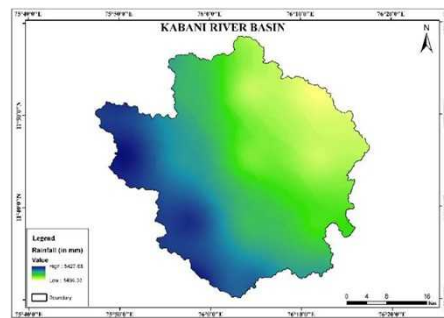


Fig 4g : Rainfall, source: IMD IMDAA Era 5

4.1.9 Distance to Lineaments

The distance from the Lineaments map was obtained prepared from the Geological Survey of India (GSI). The relationship between the lineament distance and landslides was determined found out using <200, 200–400, 400–600, 600–800, and >800 m, and the distance between the lineaments was calculated using the Euclidean distance due to the risk of slope the imbalance of slope.

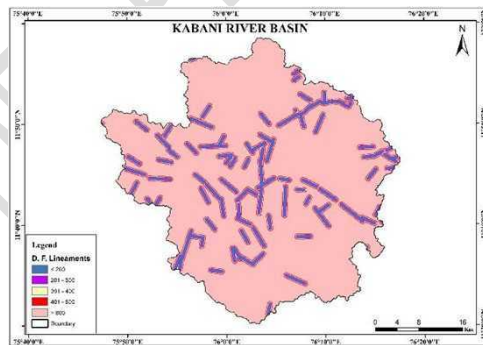


Figure. 4h : Lineaments, source: Geological Survey of India

4.1.10 Distance to Roads

Road construction is a human-made process cut and creation that causes slope instability (Bui et al., 2011). Road construction with a steeper slopes is associated with a higher risk of accidents. Owing Due to the potential for slope instability, the distance between roads was calculated using Euclidean distance. The

study area was classified into five groups based on the distances such from the road as: <100, 101-200, 201-300, 301-500 and >500 based on the distance from the road.

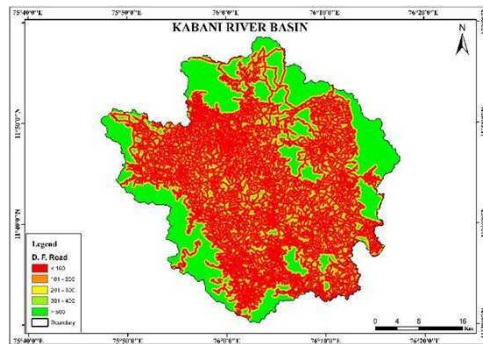


Fig. 4i: Road, source: Open Series Map

Commented [SA11]: Distance to roads

1.1.1 Distance to Streams

Rivers in a watershed are the result of long-term interactions between creations that trigger slope instability, geographical features in the impact of water, and topography, and slope (Bui et al., 2011). The distance from the streams is one of the proximity parameters, and the distance between the streams is calculated using the Euclidean distance because due to the risk of slope the instability of the slopes. They we are classified as into <100, 101-200, 201-300, 301-500, and >500 (Fig. 4j) for the analysis.

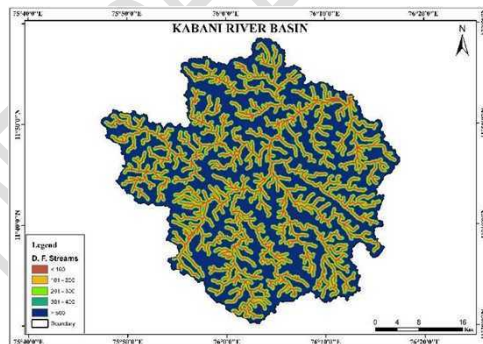


Fig. 4j: Rivers, source: SRTM DEM

Commented [SA12]: Distance to streams

1.2 Analysis of the factors influencing landslides

The frequency ratio and prediction rate for all classes were obtained from all the prepared conditioning factors of the training dataset. The ratio of landslides and domains, frequency ratio, relative frequency, and prediction rate for each class and factor are is displayed in Table 5a. The F frequency ratios are is frequently used in landslide susceptibility studies research. However, in this case, standardizsation between 0 and 1 was applied to allow for a better comparison and understanding of the impact on the LSI calculation. As

such, the prediction rate [provides offers](#) a weighting of the variables that affect the landslide susceptibility index.

Table. 1: The ratio of landslides and domains, frequency ratio, relative frequency, and prediction rate for each class and factor

	Count	<i>F_{nij}</i>	Previous	<i>FL_{ij}</i>	<i>W_{ij}</i>	FR
CURVATURE						
Concave	638464	0.34106	107	0.601	1.762	176.2
Flat	638256	0.34095	35	0.196	0.576	57.67
Convex	595256	0.31798	36	0.202	0.636	63.6
LU/LC						
Agriculture	225015	0.12018	38	0.213	1.776	177.6
Tea	92970	0.04965	15	0.084	1.697	169.7
Paddy	20410	0.0109	1	0.005	0.515	51.53
Rocky	80326	0.0429	6	0.033	0.785	78.57
Built-up	10350	0.00553	2	0.011	2.032	203.2
Deciduous Forest	390954	0.2088	26	0.146	0.699	69.95
Coffee (agroforestry)	764104	0.4081	79	0.443	1.087	108.7
Evergreen Forest	221525	0.11831	10	0.056	0.474	47.48
Water body	19367	0.01034	0	0	0	0
Forest Plantation	4829	0.00258	0	0	0	0
H.A Grasslands	23747	0.01268	1	0.005	0.442	44.29
Tree plantation	18764	0.01002	0	0	0	0
SOILTEXTURE						
Clay	1299961	0.69429	142	0.797	1.149	114.9
Loam	343856	0.18365	6	0.033	0.183	18.35
Gravelly Clay	211215	0.11281	12	0.067	0.597	59.76
Gravelly Loam	17328	0.00926	18	0.101	10.92	1092
GEOMORPHOLOGY						
Pediment	10966	0.00586	1	0.005	0.959	95.92
Valley Fill	378476	0.20214	23	0.129	0.639	63.92
Water Body - River	27079	0.01446	3	0.016	1.165	116.5
Rolling Plain	935137	0.49944	72	0.404	0.809	80.98
Active Quarry	320	0.00017	0	0	0	0
Residual Mound	39361	0.02102	3	0.016	0.801	80.17
Pedi plain	9791	0.00523	0	0	0	0
Channel Bar	2625	0.0014	0	0	0	0
Residual Hill	2808	0.0015	0	0	0	0
Plateau Remnant	10505	0.00561	0	0	0	0
Ridge	4584	0.00245	0	0	0	0
Hills and Valleys	450709	0.24072	76	0.426	1.773	177.3
LITHOLOGY						

Commented [SA13]: If you are mentioning curvature, then why in above image it is mentioned "Slope curvature".

Commented [SA14]: Rewrite as "LULC"

Garnet-Sillimanite- Gneiss	50951	0.02725	0	0	0	0
Sericite Schist	97442	0.05211	4	0.022	0.431	43.12
Amphibolite	5520	0.00295	0	0	0	0
Pink Granite	14909	0.00797	0	0	0	0
Diorite	52066	0.02784	5	0.028	1.008	100.8
Granite Gneiss	1172789	0.62712	61	0.342	0.546	54.64
Grey Hornblende	136386	0.07293	30	0.168	2.31	231
Biotite Gneiss				539	995	995
Talc Tremolite Actinolite	13629	0.00729	1	0.005	0.77	77.08
Schist				618	874	744
Pegmatite	127	6.79E-05	0	0	0	0
Quartz Vein/Reef	2295	0.00123	1	0.005	4.577	457.7
Acid to Intermediate	252525	0.13503	74	0.415	3.078	307.8
Charnockite				73	754	754
Silimanite-Kyanite-	345	0.00018	0	0	0	0
Quartz Schist						
Anorthosite Gabbro	66526	0.03557	1	0.005	0.157	15.79
Graphite-Biotite Schist	1646	0.00088	1	0.005	6.382	638.2
Fuchsite-Kyanite	2956	0.00158	0	0	0	0
Quartzite						
SLOPE ANGLE						
0-5	583398	0.31165	9	0.05	0.162	16.22
5.1-10	644301	0.34418	41	0.23	0.669	66.92
10.1-20	498176	0.26612	96	0.539	2.026	202.6
20.1-30	117967	0.06302	30	0.168	2.674	267.4
30.1-40	25976	0.01388	2	0.011	0.809	80.97
> 40.1	2158	0.00115	0	0	0	0
RAINFALL						
< 2,500	540558	0.2887	0	0	0	0
2,501 - 3,500	527551	0.28176	21	0.117	0.418	41.87
> 3,500	804252	0.42954	157	0.882	2.053	205.3
TWI						
Low	1158069	0.61864	146	0.82	1.325	132.5
Medium	584369	0.31217	31	0.174	0.557	55.78
High	129515	0.06919	1	0.005	0.081	8.119
DISTANCE FROM STREAMS						
Very Near	300503	0.16049	34	0.191	1.19	119
Near	253602	0.13545	25	0.14	1.036	103.6
Average	260174	0.13896	21	0.117	0.849	84.9
Far	410488	0.21924	41	0.23	1.05	105
Very Far	647594	0.34587	57	0.32	0.925	92.58
DISTANCE FROM ROAD						
Very Near	897595	0.47939	139	0.78	1.628	162.8

Commented [SA15]: Previously, it is mentioned "Distance to Streams". Kindly make it uniform throughout.

Near	333893	0.17833	19	0.106	0.598	59.85
Average	145550	0.07774	14	0.078	1.011	101.1
Far	123485	0.06595	4	0.022	0.34	34.07
Very Far	371838	0.19859	2	0.011	0.056	5.657
DISTANCE FROM LINEAMENT						
Very Near	112219	0.05993	6	0.033	0.562	56.24
Near	123530	0.06598	12	0.067	1.021	102.1
Average	132972	0.07102	5	0.028	0.395	39.55
Far	129427	0.06913	3	0.016	0.243	24.38
Very Far	1374213	0.73395	152	0.853	1.163	116.3
LSI (sum of wij) = 73.61519						

Regarding the elevation factor, the area between 700 and 2028.67 metres exhibits a high RF value, which suggests that this region is susceptible to landslides and that such events have occurred more frequently in the past, particularly during periods of heavy rainfall. The RF value was greater for slopes ranging from 0° to 65.56°. Most global case studies have shown that high relief and steep slopes are primary causes of landslides (Y. Hong et al., 2007). Research indicates a distribution of landslides on flat surfaces, caused by the base of the landslide or the underlying bedrock (Cestras et al., 2022). Similarly, landslides tend to occur more often on concave slopes than on steep ones. Concave slopes often concentrate water at their lower edges; however, they are generally more stable because the water flow is more evenly distributed (Gimire & Timalisina, 2020). The TWI represents the relationship between the amount of water accumulated in a specific area and the slope of the stream (Bevan & Kirkby, 1979; Benzogag et al., 2020).

TWI also showed that landslides are likely in our scenario, with TWI ranging from 3.01 to 27.41, indicating large landslides. Because Due to the ease of construction, and slope cutting, and evacuation, especially in the study area, most roads are built on river-banks. This may be due to the high risk in the upper reaches.

Rainfall naturally causes landslides. The annual average rainfall also increases with an increase in the study area, and the relative frequency suggests that rainfall above 3312 mm is more likely to cause landslides. Because Since our region is known for its frequent rainfall events, in some areas, the possibility of landslides may occurring more frequently is possible if rainfall exceeds this figure (Sestraj et al., 2019). Finally, from a structural perspective, there is a correlation between the relative frequency values and the road crossing faults; landslides are also likely to occur in areas located within 200 m of the road, stream, and lineament.

1.3 Landslide susceptibility map and validation

The landslide susceptibility map of the Kabani River Basin displays a clear spatial pattern, where the western and southwestern regions show high and intense landslide susceptibility, as indicated by the red to orange areas. These areas certainly fit the distribution of previous landslide events, as shown as black dots on the map. In contrast, the northeastern and eastern parts of the river basin, which are green, remained relatively stable. This spatial distribution highlights the dominant influence of the topographic, climatic, and geological parameters.

One of the primary contributors to this pattern is the high rainfall in the western part, where the Kabani River Basin is located in the lee side of the Western Ghats. The region receives intense monsoon rainfall, which increases the soil saturation and reduces the slope stability. In addition, the presence of loamy soils, which retain water and become unstable when wet, renders makes this region particularly vulnerable to landslides. Loamy soils are fertile but structurally weak under saturated conditions, especially on sloping terrains. The sSloping structure is an important factor, because as sloping areas are more susceptible to gravitational movement.

The more the terrain is disturbed, the more sensitive are the sloped areas are. Steep slopes accelerate surface runoff, erosion, and the downward movement of soil and debris. This is evident in the south and southwest, where extreme susceptibility overlaps with the steep terrain. In addition, the curvature of the terrain also plays a role: concave slopes collect water and increase saturation, whereas while steep slopes may be more susceptible to mass movement.

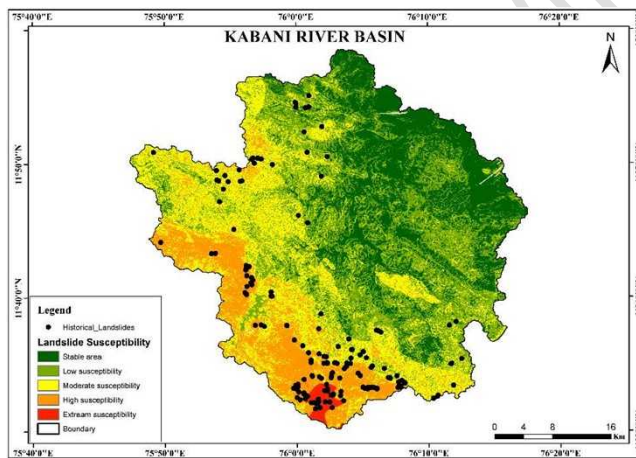


Fig. 5 : Landslide Susceptibility Map

The Topographic Wetness Index (TWI), which measures the moisture accumulation and is partially related connected to the instability of the surface. High potentials in the valleys and depressions are often associated with areas of moderate to high potential. In addition, distance to streams affects drainage and erosion processes, with areas near streams experiencing more intense subsoil erosion, and proximity to roads introducing inges man-made instability from slope cutting and construction. The gGeological and structural constraints also contributed significantly make an important contribution. The type and composition of the lithology and the bedrock influences the strength of the slope and the nature of the weathering; weaker and weathered rocks, such as phyllites or schists, are more likely to fail. Similarly, in terms of land use, different types of cultivation can accelerate landslides in some places, while simultaneously at the same time decreasing the impact of landslides in others. Distance to lineament and structural features, such as faults and fractures, can indicate areas of weakness where landslides are more likely to be initiated. Geomorphology, which includes landform classifications, such as escarpments,

pediments, and valleys, can help explain why some areas naturally initiate mass movement. For example, rugged hills and escarpments exhibit high landslide densities ~~because~~~~due~~ ~~of~~~~the~~ the instability of the area.

The integration of diverse factors, such as climatology, topography, hydrology, and geology, demonstrates a holistic approach ~~toused in the~~ vulnerability assessment, which helps to more accurately identify areas at risk in the Kabani River Basin. The correlation between ~~the~~ slope, soil type, and historical landslide locations confirms the effectiveness of this geospatial model in identifying hazardous areas, aiding disaster mitigation, and land use planning in the Kabani River Basin.

5. SUMMARY AND CONCLUSION

~~The~~ Landslide susceptibility assessment in the Kabani River Basin highlights ~~thea~~ complex interplay of natural and anthropogenic factors ~~that~~ influenceing slope stability. The western and southwestern regions, characterized by steep slopes, high rainfall, loamy and clay soils, and weak geomorphology, showed higher or more severe susceptibility than the northeastern regions. Key contributing parameters such as curvature, topographic wetness index (TWI), proximity to roads, streams, and lineaments, and lithological and geomorphological distributions and variations make ~~the~~ hazard mapping more accurate. The close alignment of past landslide events with areas identified as ~~having~~ high probability ~~particularly~~ confirms the reliability of the model. This analysis also underscores the importance of integrated geospatial approaches ~~to~~in landslide hazard zoning. Effective mitigation strategies in ~~the~~ river basins, land use planning, and infrastructure development should be prioritized for these high-risk areas to reduce potential landslides in the future.

REFERENCES

1. Abdul Rachman Rasyid^{1,2*}, Netra P. Bhandary¹ and Ryuichi Yatabe¹ "Performance of frequency ratio and logistic regression model in creating GIS-based landslides susceptibility map at Lompobattang Mountain, Indonesia" Rasyid et al. *Geoenvironmental Disasters* (2016) 3:19 DOI 10.1186/s40677-016-0053-x
2. Abidi, A., Demehati, A. & El Qandil, M. Landslide Susceptibility Assessment Using Evidence Belief Function and Frequency Ratio Models in Taounate city (North of Morocco). *Geotech Geol Eng* 37, 5457–5471 (2019). <https://doi.org/10.1007/s10706-019-00992-0>
3. Achu AL, Aju CD, Reghunath R (2020) Spatial modelling of shallow landslide susceptibility: a study from the southern Western Ghats region of Kerala, India. *Ann GIS*, 1–19. <https://doi.org/10.1080/19475683.2020.1758207>
4. Achu, A. L., Thomas, J., Aju, C. D., Gopinath, G., Kumar, S., & Reghunath, R. (2021). Machine-learning modelling of fire susceptibility in a forest-agriculture mosaic landscape of southern India. *Ecological Informatics*, 64, 101348.
5. Anbazhagan S, Sajinkumar KS (2011) Geoinformatics in terrain analysis and landslide susceptibility mapping in parts of Western Ghats, India. *Geoinformatics in applied geomorphology*. CRC Press, Boca Raton, pp 291–315
6. Ankur Sharma¹ · Har Amrit Singh Sandhu¹ · Claudia Cherubini², "Enhanced landslide susceptibility zonation using GIS-Based ensemble Techniques" *Environmental Earth Sciences* (2025) 84:37 <https://doi.org/10.1007/s12665-024-12032-z>
7. Benzougagh, B., Meshram, S.G., Baamar, B. et al. (2020).. Relationship between landslide and morpho-structural analysis: a case study in the Northeast of Morocco. *Appl Water Sci* 10, 175 (2020). <https://doi.org/10.1007/s13201-020-01258-4>.
8. Beven KJ, Kirkby MJ (1979) A physically based, variable contributing area model of basin hydrology/Un modèle à base physique de zone d'appel variable de l'hydrologie du bassin versant. *Hydrol Sci J* 24(1):43–69. <https://doi.org/10.1080/02626667909491834>
9. Bilaşco, Ş., Roşca, S., Vescan, I., Fodorean, I., Dohotar, V., Sestras, P., 2021. A GIS-based spatial analysis model approach for identification of optimal hydrotechnical solutions for gully erosion stabilisation. *Case Study. Appl. Sci.* 11 (11), 4847. <https://doi.org/10.3390/app11114847>.
10. Bui, D.T., Lofman, O., Revhaug, I., Dick, O., 2011. Landslide susceptibility analysis in the Hoa Binh province of Vietnam using statistical index and logistic regression. *Nat. Hazards* 59 (3), 1413–1444. <https://doi.org/10.1007/s11069-011-9844-2>.
11. Cao, C., Chen, J., Zhang, W., Xu, P., Zheng, L., & Zhu, C. (2019). Geospatial Analysis of Mass-Wasting Susceptibility of Four Small Catchments in Mountainous Area of Miyun County,

- Beijing. International Journal of Environmental Research and Public Health, 16(15), 2801. <https://doi.org/10.3390/ijerph16152801>
12. Chen W, Shahabi H, Shirzadi A, Li T, Guo C, Hong H, Li W, Pan D, Hui J, Ma M, Xi M (2018) A novel ensemble approach of bivariate statistical-based logistic model tree classifier for landslide susceptibility assessment. *Geocarto Int* 1–23. <https://doi.org/10.1080/10106049.2018.1425738>
 13. Chung CJF, Fabbri AG (1999) Probabilistic prediction models for landslide hazard mapping. *Photogramm Eng Remote Sens* 65(12):1389–1399
 14. D. Nagaraju and C. Papanna (2009) Hydrogeochemical Studies of Kabini River Basin, Karnataka, India vol.8, no.1, pp.111-118
 15. Devkota KC, Regmi AD, Pourghasemi HR, Yoshida K, Pradhan B, Ryu IC, Dhital MR, Althuwaynee OF (2013) Landslide susceptibility mapping using certainty factor, index of entropy and logistic regression models in GIS and their comparison at Mugling-Narayanghat road section in Nepal Himalaya. *Nat Hazards* 65(1):135–165. <https://doi.org/10.1007/s11069-012-0347-6>
 16. Gerrard J (1994) The landslide hazard in the Himalayas: geological control and human action. *Geomorphology* 10(1–4):221–230. [https://doi.org/10.1016/0169-555X\(94\)90018-3](https://doi.org/10.1016/0169-555X(94)90018-3)
 17. Ghimire, M., Timalisina, N., 2020. Landslide Distribution and Processes in the Hills of Central Nepal: Geomorphic and Statistical Approach to Susceptibility Assessment. *J. Geosci. Environ. Protection* 08 (12), Article 12. <https://doi.org/10.4236/gep.2020.812017>.
 18. Glade T, Anderson M, Crozier MJ (Eds.) (2005) *Landslide Hazard and Risk*. Wiley. <https://doi.org/10.1002/9780470012659>
 19. Gregory C. Ohlmacher Plan curvature and landslide probability in regions dominated by earth flows and earth slides *Engineering Geology* 91 (2007) 117–134
 20. Haque U, da Silva PF, Devoli G, Pilz J, Zhao B, Khaloua A, Wilopo W, Andersen P, Lu P, Lee J, Yamamoto T, Keellings D, Wu J-H, Glass GE (2019) The human cost of global warming: Deadly landslides and their triggers (1995–2014). *Sci Total Environ* 682:673–684. <https://doi.org/10.1016/j.scitotenv.2019.03.415>
 21. Hawas Khan a, Muhammad Shafique b,†, Muhammad A. Khan a, Mian A. Bacha b, Safeer U. Shah b, Chiara Calligaris c ,Landslide susceptibility assessment using Frequency Ratio, a case study of northern Pakistan, *The Egyptian Journal of Remote Sensing and Space Sciences* 22 (2019) 11–24
 22. Hong, Y., Adler, R., Huffman, G., 2007. Use of satellite remote sensing data in the mapping of global landslide susceptibility. *Nat. Hazards* 43 (2), 245–256. <https://doi.org/10.1007/s11069-006-9104-z>.

23. Kavzoglu, T., Sahin, E.K. & Colkesen, I. Landslide susceptibility mapping using GIS-based multi-criteria decision analysis, support vector machines, and logistic regression. *Landslides* 11, 425–439 (2014). <https://doi.org/10.1007/s10346-013-0391-7>
24. Kayastha P, Dhital MR, De Smedt F (2013) Application of the analytical hierarchy process (AHP) for landslide susceptibility mapping: a case study from the Tinau watershed, west Nepal. *Comput Geosci* 52:398–408. <https://doi.org/10.1016/j.cageo.2012.11.003>
25. Krishnan MVN, Pratheesh P, Rejith PG, Vijith H (2015) Determining the suitability of two different statistical techniques in shallow landslide (debris flow) initiation susceptibility assessment in the western Ghats. *Environ Res Eng Manag* 70(4):26–39. <https://doi.org/10.5755/j01.ere.m.70.4.8510>
26. Kumar BM (2006) Land use in Kerala: changing scenarios and shifting paradigms. *J Trop Agric* 43:1–12
27. Kuriakose SL, Sankar G, Muraleedharan C (2009) History of landslide susceptibility and a chorology of landslide-prone areas in the Western Ghats of Kerala India. *Environ Geol* 57(7):1553–1568. <https://doi.org/10.1007/s00254-008-1431-9>
28. Lee S, Sambath T (2006) Landslide susceptibility mapping in the Damrei Romel area, Cambodia using frequency ratio and logistic regression models. *Environ Lithol* 50(6):847–855. <https://doi.org/10.1007/s00254-006-0256-7>
29. Lee, S., Pradhan, B. Landslide hazard mapping at Selangor, Malaysia using frequency ratio and logistic regression models. *Landslides* 4, 33–41 (2007). <https://doi.org/10.1007/s10346-006-0047-y>
30. Merghadi A, Yunus AP, Dou J, Whiteley J, ThaiPham B, Bui DT, Avtar R, Abderrahmane B (2020) Machine learning methods for landslide susceptibility studies: A comparative overview of algorithm performance. *Earth Sci Rev* 207:103225. <https://doi.org/10.1016/j.earscirev.2020.103225>
31. Meten M, PrakashBhandary N, Yatabe R (2015) Effect of landslide factor combinations on the prediction accuracy of landslide susceptibility maps in the Blue Nile Gorge of Central Ethiopia. *Geoenvironmental Disasters* 2(1):9. <https://doi.org/10.1186/s40677-015-0016-7>
32. N. R. Anoop and T. Ganesh., 2023. The Forests and Elephants of Wayanad: Challenges for Future Conservation ,DOI: 10.18520/cs/v118/i3/362-367
33. Sestras, P., Bilaşco, Ş., Roşca, S., Ilies, N., Hysa, A., Spalević, V., Cîmpeanu, S.M., 2022. Multi-instrumental approach to slope failure monitoring in a landslide susceptible newly built-up area: Topo-Geodetic survey, UAV 3D modelling and ground-penetrating radar. *Remote Sens. (Basel)* 14 (22), 5822. <https://doi.org/10.3390/rs14225822>.

34. Sharma S, Mahajan AK (2018) A comparative assessment of information value, frequency ratio and analytical hierarchy process models for landslide susceptibility mapping of a Himalayan watershed, India. *Bull Eng Lithol Environ* 1–18. <https://doi.org/10.1007/s10064-018-1259-9>
35. Sonker, Irjesh & Tripathi, Jayant & Maurya, Swarnim. (2022). Remote sensing and GIS-based landslide susceptibility mapping using frequency ratio method in Sikkim Himalaya. *Quaternary Science Advances*. 8. 100067. [10.1016/j.qsa.2022.100067](https://doi.org/10.1016/j.qsa.2022.100067).
36. SSO (2007) Benchmark soils of Kerala. Soil Survey Organization, Government of Kerala, Thiruvananthapuram
37. Thampi PK, Mathai J, Sankar G (1995) A regional evaluation of landslide prone areas in the Western Ghats of Kerala. In: Abstracts of the national seminar on landslides in Western Ghats, 29–30 Aug 1995. Centre for Earth Science Studies, Government of Kerala, Thiruvananthapuram, India
38. Tien Bui D, Pradhan B, Lofman O, Revhaug I, Dick OB (2012) Landslide susceptibility mapping at Hoa Binh province (Vietnam) using an adaptive neuro-fuzzy inference system and GIS. *Comput Geosci* 45:199–211. <https://doi.org/10.1016/j.cageo.2011.10.031>
39. Vijith H, Madhu G (2008) Estimating potential landslide sites of an upland sub-watershed in Western Ghat's of Kerala (India) through frequency ratio and GIS. *Environ Lithol* 55(7):1397–1405. <https://doi.org/10.1007/s00254-007-1090-2>
40. Walker LR, Shiels AB (2013) Physical causes and consequences for Landslide Ecology
41. Zhang, Z., Yang, F., Chen, H. et al. GIS-based landslide susceptibility analysis using frequency ratio and evidential belief function models. *Environ Earth Sci* 75, 948 (2016). <https://doi.org/10.1007/s12665-016-5732-0>
42. Zizheng Guo a, Yu Shi b, Faming Huang b,†, Xuanmei Fan c, Jinsong Huang d ,2021, Landslide susceptibility zonation method based on C5.0 decision tree and K-means cluster algorithms to improve the efficiency of risk management.